Transition from traveling to standing waves in the 4:1 resonant Belousov-Zhabotinsky reaction

Bradley Marts and Anna L. Lin*
Center for Nonlinear and Complex Systems and Department of Physics, Duke University, Durham, North Carolina 27708, USA
(Received 19 June 2007; published 14 February 2008)

We report a transition from traveling to standing domain walls in a parametrically forced two-dimensional oscillatory Belousov-Zhabotinsky chemical reaction in 4:1 resonance. Our experimental results demonstrate spatiotemporal solutions not predicted by previous analytic results of the complex Ginzburg-Landau amplitude equation and numerical results from reaction-diffusion models. In addition to the stationary π fronts at high forcing amplitudes, the 4:1 resonant patterns we observe include stationary $\pi/2$ fronts.

DOI: 10.1103/PhysRevE.77.026211 PACS number(s): 05.45.Xt, 82.40.Ck, 82.40.Bj, 05.65.+b

I. INTRODUCTION

When a spatially extended system has multiple equivalent states, e.g., the spin states in a magnetic system [1], the orientation of liquid crystals [2], or the phases of light in an optical cavity [3], the system can form spatial domains of distinct states separated from each other by domain walls. In nonequilibrium systems, traveling domain wall solutions can be asymptotically stable [4] because the dynamics are not governed by energy minimization. Transitions between traveling and stationary waves in periodically forced oscillatory systems have been studied, for example, in nematic liquid crystals and binary mixture convection [5], and theoretically using amplitude equations [6] and reaction-diffusion equations [7]. In this paper, we report on an experimental demonstration of a bifurcation from traveling to stationary domain walls in the 4:1 resonant Belousov-Zhabotinsky (BZ) chemical reaction. The stationary domain walls we observe are not yet found in analysis of the forced complex Ginzburg-Landau (FCGL) equation or reaction-diffusion models [8,9].

We observe these stationary 4:1 resonant fronts in a time-periodic quasi-two-dimensional (2D) BZ chemical reaction that is externally forced with a frequency close enough to four times its natural oscillation frequency to cause the reaction to become phase synchronized to $\frac{1}{4}$ the forcing frequency. The result is a subharmonic 4:1 resonance characterized by a response frequency that is exactly $\frac{1}{4}$ of the forcing frequency and four distinct but equivalent temporal oscillations shifted in phase by $\pi/2$ and separated in space by domain walls. The strength of the external forcing is the control parameter; the change in stability from traveling to stationary walls occurs as the strength of the external forcing is increased. A large forcing strength results in standing waves, while a small forcing strength results in traveling waves.

The bifurcation we report is similar to the well known nonequilibrium Ising-Bloch (NIB) bifurcation found in 2:1 resonance, where stationary Ising walls become unstable to traveling Bloch walls [4,10,11]. For both the NIB and the bifurcation in 4:1 resonance, the temporal dynamics of the domain walls are intrinsically linked with the instantaneous spatial structure. Domain walls that are stationary in time are characterized by the existence of a zero-amplitude node in space while domain walls that travel do not have a spatial node.

The details of the experimental setup, data acquisition, and data analysis are in Secs. II and III. Our experimental observations are given in Sec. IV. We compare these to existing theoretical work in Sec. V and demonstrate the existence of a spatiotemporal solution in our experiments not previously predicted by either the FCGL or reaction-diffusion equations.

II. EXPERIMENTAL SETUP

We use the same BZ reactor setup reported in [12–14]. The reaction takes place in a thin porous Vycor glass membrane sandwiched between two chemical reservoirs. The glass membrane is 0.4 mm thick and 22 mm in diameter. Reagents diffuse homogeneously from the continuously stirred reservoirs into the glass through its two faces. The chemical concentrations in one reservoir are $0.8M$ sulfuric acid, $0.184M$ potassium bromate, and $0.001M$ tris(2, 2′-bipyridyl)dichlororuthenium(II)hexahydrate; and in the other $0.8M$ sulfuric acid, $0.184M$ potassium bromate, $0.32M$ malonic acid, and $0.3M$ sodium bromide. The pattern wavelength is $\geqslant$0.5 mm while the membrane is 0.4 mm thick, so the pattern is quasi-two-dimensional. We use a ruthenium-catalyzed version of the reaction with reagent concentrations such that the reaction is oscillatory. The natural period of spatially homogeneous oscillations is roughly 34 s.

The ruthenium catalyst of the BZ chemical reaction is light sensitive in the visible range [15]. To force the system, we apply time-periodic spatially uniform pulses of light to the membrane. The particular effects of light using the same reactor setup we use here have been described previously [14]. The parametric forcing is applied using a computer-controlled commercial video projector.

We image the reaction by passing spatially homogeneous low-intensity light through the membrane, and measure the relative intensity of the transmitted light (optical density) using a charge-coupled device (CCD) camera ($\sim$13 pixels/mm) bandpass filtered from 420 to 500 nm. Regions of the glass membrane that contain Ru(II) absorb light at 451 nm, so regions of high intensity have a lower concentration of Ru(II). We create a temporal movie of the

*alin@phy.duke.edu

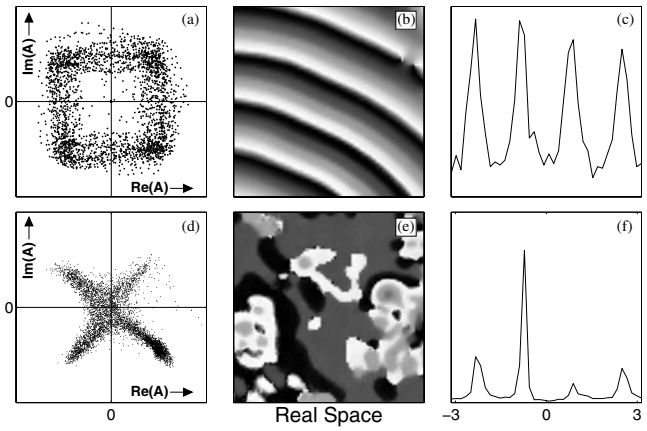

FIG. 1. (a), (d) Complex Fourier coefficient A, given by Eq. (2), is plotted as a point in the complex plane for each pixel from the camera data. The absolute scale of the axes is arbitrary, but is the same in (a) and (d). (b), (e) Phase of the complex amplitude A is with a periodic gray scale. The axes are the real space axes from the 2D experiment. (a)–(c) 4:1 traveling pattern at low forcing amplitude. Phase image is 5.7×5.7 mm^2. (d)–(f) Standing wave pattern in the 4:1 resonance. The complex amplitude has a zero-amplitude node separating spatial domains. Phase image is 11.9×11.9 mm^2. Chemical conditions are given in Sec. II.

ruthenium oscillations by capturing frames from the camera every 2 s.

III. DATA ANALYSIS

We quantify the temporal oscillations using the complex Fourier amplitude $A(t,\vec{x})=re^{i\delta}$, where r is the oscillation magnitude and δ is the (relative) phase. A complex plane portrait is constructed as in previous work [13] by plotting the point A in the complex plane at a fixed time for each pixel in the movie. An example of complex plane portraits can be seen in the left column of Fig. 1. We visualize the pattern in real space by plotting the phase δ at each pixel (see the center column of Fig. 1). The usefulness of A is evident by the topological change in the complex plane portrait from a square for the traveling four-phase pattern (top) at low forcing strength to a cross for the stationary four-phase pattern (bottom) at higher forcing strength. Interpretations of the complex plane portraits are given in Secs. IV and V.

We obtain the complex Fourier amplitude from the experimental data following previously successful methods [13]. For clarity we include here the explicit transformation from the experimental data to the complex amplitude.

In the optical density measurements captured with a CCD camera, the time-varying intensity at a single pixel is proportional to the time-dependent chemical concentration at that pixel. To extract the complex amplitude of the temporal chemical oscillation at each pixel we use a Fourier analysis to filter in frequency space in the following way. The intensity of transmitted light C is measured at discrete intervals nT, where $n=0,1,\ldots,N-1$ and $T=2$ s. We use a discrete Fourier transform to obtain the frequency of this signal, $\tilde{C}$, at frequencies $m\Omega$, $m=0,1,\ldots,N-1$, $\Omega=[2T(N-1)]^{-1}$:

$$\tilde{C}(m\Omega,\vec{x})=\sum_{k=0}^{k=N-1}C(kT,\vec{x})e^{-2\pi imk/N}. \quad (1)$$

The inverse transform is carried out only for frequencies within an interval spanning the resonance frequency, $((n-n_0)\Omega,(n+n_0)\Omega)$, and the oscillation at the resonance frequency, $n\Omega$, is divided out:

$$A(kT,\vec{x})=\frac{e^{-2\pi ink/N}}{N}\sum_{m=n-n_0}^{m=n+n_0}\tilde{C}(m\Omega,\vec{x})e^{2\pi imk/N}, \quad (2)$$

leaving the complex amplitude $A=re^{i\delta}$. We choose the filter width just large enough to observe any slow changes in the magnitude and phase of the oscillations that contributes to Fourier components at frequencies slightly above and below the resonance frequency. It is important to capture the slow changes in the complex amplitude as they will be present as a result of traveling waves.

IV. EXPERIMENTAL RESULTS

We have observed in our experimental system a transition from traveling to standing domain walls. A traveling pattern similar to those reported previously [9] is shown in Fig. 1 (top row). The traveling waves form four armed rotating spirals shown by the four shades of gray in the real space image. Each of the four arms oscillates at the same frequency but at distinct phases that differ from their spatial neighbors by $\pi/2$—thus the walls between them are called "$\pi/2$ walls." The second row of Fig. 1 shows a standing wave pattern at 4:1 resonance. This pattern occurs for larger external forcing strengths than the traveling wave. The domain walls in this pattern are stationary [16], all four phases are present, and neighboring domains differ by either π or $\pi/2$. That is, there are both stationary π and $\pi/2$ walls.

The transition from traveling to standing patterns is most strikingly observed in the complex plane portraits (see the left column of Fig. 1). The traveling waves form a square pattern in the complex plane with the majority of the pattern contributing to the four equivalent phases at the corners of the square. The standing wave forms a cross pattern in the complex plane. The majority of the pattern is at high amplitude, but the domains are connected by walls with zero-amplitude oscillations. The topological structure seen in the complex plane portrait snapshots is intrinsically linked with the traveling and standing wave temporal dynamics of each pattern.

The complex plane portraits reveal both the fourfold symmetry of the four stable states and the spatial structure of domain walls between them. For the traveling pattern, domains contribute to the corners of the square, which oscillate at the four phase-locked phases, and domain walls contribute to the sides of the square, which oscillate out of phase with the resonant response. As the spatial pattern is traversed from one domain to the next at a snapshot in time, there is a continuous rotation of the phase. For successive snapshots in time, the domain wall travels, and the points along the side of the square move into one of the corners while a few points from the corners move into the sides. As successive domain

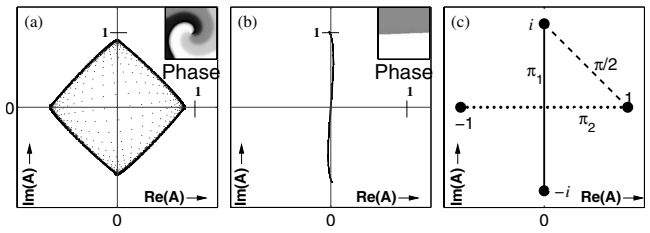

FIG. 2. (a) Traveling spiral waves in the FitzHugh-Nagumo simulation. (b) Standing wave pattern at larger forcing strength. FitzHugh-Nagumo parameters are the same as in [9]. (c) Schematic of the complex plane representation of the four equivalent states and spatial solutions connecting them.

walls pass a particular pixel in the image, the point in the complex plane portrait representing that pixel travels along the sides of the square stopping in each corner before the next domain wall passes.

The spatial structure and dynamics of the standing walls revealed by the complex plane portrait differ significantly from those of the traveling walls. Domain walls in the standing pattern connect neighboring domains through zero amplitude nodes. Instead of the continuous change in the oscillation phase observed in the traveling patterns, the phase changes abruptly by π or $\pi/2$. Successive snapshots in time reveal that the domain walls are stationary—points in the complex remain at the same phase. The standing domain walls are formed depending on the essentially random initial conditions of the experiment. There is no long-range spatial correlation for these domain walls. This is in contrast with the traveling walls, which are organized as spiral patterns around a pacemaker center.

V. DISCUSSION

Theoretical results have never reported the cross shape in Fig. 1 (bottom) that we observe in our experiments. Both reaction-diffusion equations and the FCGL have been used to show the transition from traveling to standing waves and in both cases only stationary π walls are reported as asymptotically stable beyond the transition to standing waves [8]. While it is possible to have a cross shape complex plane portrait made of two π walls, it is not possible to arrange the walls in real space without requiring a stationary $\pi/2$ wall as well. In the experiment, we observe stationary $\pi/2$ walls in addition to both types of π walls.

We have reproduced the simulations reported in [9] for the FitzHugh-Nagumo equations in order to clearly compare the results of the theoretical approach to our experimental results [17]. The results of this simulation can be seen in Fig. 2. Similar to the experiment, traveling patterns in the simulation appear as four armed spirals where neighboring arms are shifted in phase by $\pi/2$. The walls that separate these domains oscillate out of phase with the resonance response. The resulting shape in the complex plane is a square. Standing wave patterns consist of domains shifted by π. The π walls have a zero-amplitude node between the two uniformly oscillating spatial regions and everywhere oscillate with the resonant phase. Unlike in the experiment, stationary $\pi/2$ walls are not present in the simulation.

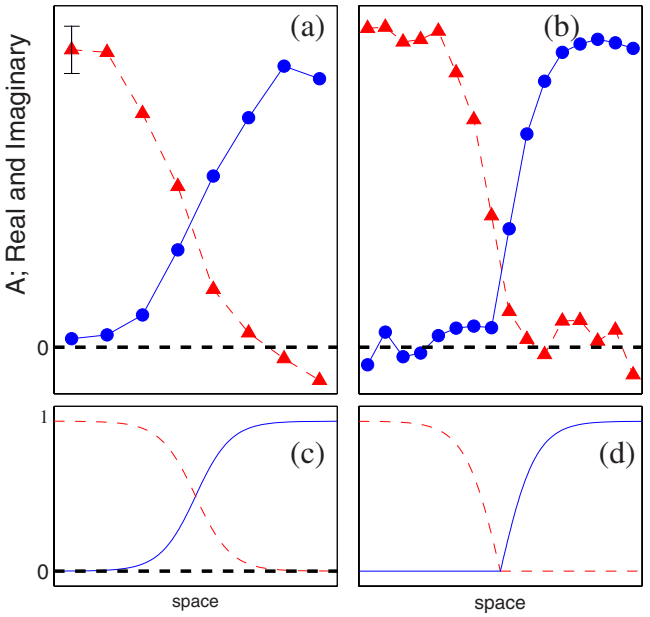

FIG. 3. (Color online) In all plots the dashed curve is the real part of the complex amplitude A and the solid curve is the imaginary part. Top: Experimental traveling (a) and stationary (b) $\pi/2$ walls. The scale on the vertical axes is arbitrary, but it is the same in both (a) and (b). (c) Theoretical $\pi/2$ wall given in Eq. (3) obtained by solving the related gradient case. (d) Proposed form of the stationary $\pi/2$ wall made piecewise from two π walls, Eq. (6). This solution has a node at the center, as we observe in the experiment.

The stability of π and $\pi/2$ wall solutions has been studied analytically using the FCGL by considering the related gradient problem [8]. Figure 2(c) shows the four resonant states of complex amplitude 1, i, -1, and $-i$ with phases 0, $\pi/2$, π, and $3\pi/2$, respectively, as filled circles. The solution in space connecting two states was given in [8]; for the $\pi/2$ wall (dashed line),

$$A(x) = \frac{1}{2}[1 + i - (1 - i)\tanh(x)], \tag{3}$$

and for the π walls (solid and dotted lines),

$$A(x) = \begin{cases} \tanh(x) & (-1 \to 1, \pi_1), \quad (4) \\ i\tanh(x) & (-i \to i, \pi_2). \quad (5) \end{cases}$$

The standing wave patterns at large forcing strength in the experiment deviate from the analytic predictions. We observe $\pi/2$ walls that do not fit the form in Eq. (3) and Fig. 2(c). The stationary $\pi/2$ walls in the experiment do not connect the states 1 and i with a straight line in the complex plane, as depicted by the dashed line representing the $\pi/2$ wall in Fig. 2(c). Instead, they follow first the dotted line coinciding with the π wall labeled π_2 and at the origin begin to follow the solid line coinciding with the other π wall. That is, the state 1 is connected to the state i by following the wall π_2 from 1 to the origin and following the wall π_1 from the origin to i. Explicitly,

$$A(x) = \begin{cases} -\tanh(x) & \text{for } x < 0, \\ i\tanh(x) & \text{for } x > 0. \end{cases} \quad (6)$$

$A(x)$ is a wall solution of the gradient case, except at the origin, where it is not differentiable.

A comparison of the observed experimental walls and their theoretical counterparts as a function of space is given in Fig. 3. The real and imaginary parts of the complex amplitude are shown for the experiment in the top row, the analytically calculated $\pi/2$ wall in the bottom left, and the form of a $\pi/2$ wall given in Eq. (6) in the bottom right. Because the presence of a node in the complex amplitude where both the real and imaginary parts are zero is directly linked with a stationary wall, finding wall solutions such as the kind in Eq. (6) in the theory may lead to a more complete understanding of the observed patterns.

ACKNOWLEDGMENTS

We thank Aric Hagberg and Ehud Meron for helpful discussions, and we acknowledge support from NSF Grant No. DMR-03-48910.

[1] C Kittel, Rev. Mod. Phys. **21**, 541 (1949).
[2] G. D. Boyd, J. Cheng, and P. D. T. Ngo, Appl. Phys. Lett. **36**, 556 (1980); H. L. Ong, R. B. Meyer, and A. J. Hurd, J. Appl. Phys. **55**, 2809 (1984); J.-H. Kim, M. Yoneya, and H. Yokoyama, Nature (London) **420**, 159 (2002).
[3] K. Staliunas, *Transverse patterns in nonlinear optical resonators* (Springer, New York, 2003), Vol. 183.
[4] P. Coullet, J. Lega, B. Houchmanzadeh, and J. Lajzerowicz, Phys. Rev. Lett. **65**, 1352 (1990).
[5] I. Rehberg, S. Rasenat, J. Fineberg, M. de la Torre Juarez, and V. Steinberg, Phys. Rev. Lett. **61**, 2449 (1988).
[6] H. Riecke, J. D. Crawford, and E. Knobloch, Phys. Rev. Lett. **61**, 1942 (1988).
[7] M. Silber, H. Riecke, and L. Kramer, Physica D **61**, 260 (1992).
[8] C. Elphick, A. Hagberg, and E. Meron, Phys. Rev. Lett. **80**, 5007 (1998); C. Elphick, A. Hagberg, and E. Meron, Phys. Rev. E **59**, 5285 (1999).
[9] A. L. Lin, A. Hagberg, A. Ardelea, M. Bertram, H. L. Swinney, and E. Meron, Phys. Rev. E **62**, 3790 (2000).
[10] M. Bode, A. Reuter, R. Schmeling, and H.-G. Purwins, Phys. Lett. A **185**, 70 (1994).
[11] A. Hagberg and E. Meron, Nonlinearity **7**, 805 (1994).
[12] V. Petrov, Q. Ouyang, and H. L. Swinney, Nature (London) **388**, 655 (1997).
[13] A. L. Lin, M. Bertram, K. Martinez, H. L. Swinney, A. Ardelea, and G. F. Carey, Phys. Rev. Lett. **84**, 4240 (2000).
[14] K. Martinez, A. L. Lin, R. Kharrazian, X. Sailer, and H. L. Swinney, Physica D **168**, 1 (2002).
[15] S. Kadar, T. Amemiya, and K. Showalter, J. Phys. Chem. A **101**, 8200 (1997).
[16] Stationary walls remain fixed in space on the time scale of our experiments, 10–100 s of oscillations. There may exist some motion due to curvature, but they do not propagate like the traveling walls.
[17] The Brusselator was also integrated in [9] with similar results.